

Article

Not peer-reviewed version

# Solvothermal Synthesis of $\text{LaF}_3\text{:Ce}$ Nanoparticles for Use in Medicine: Luminescence, Morphology and Surface Properties

[Dorokhina Anastasiia](#)<sup>\*</sup>, Ryoya Ishihara, Hiroko Kominami, [Vadim Bakhmetyev](#), [Maxim Sychov](#), Toru Aoki, Hisashi Morii

Posted Date: 19 January 2023

doi: 10.20944/preprints202301.0351.v1

Keywords: X-ray luminescence; solvothermal synthesis;  $\text{LaF}_3\text{:Ce}$ ; Zeta-potential; PEG; PVP; PEI



Preprints.org is a free multidiscipline platform providing preprint service that is dedicated to making early versions of research outputs permanently available and citable. Preprints posted at Preprints.org appear in Web of Science, Crossref, Google Scholar, Scilit, Europe PMC.

Copyright: This is an open access article distributed under the Creative Commons Attribution License which permits unrestricted use, distribution, and reproduction in any medium, provided the original work is properly cited.

## Article

# Solvothermal Synthesis of LaF<sub>3</sub>:Ce Nanoparticles for Use in Medicine: Luminescence, Morphology and Surface Properties

Anastasiia Dorokhina <sup>1,2,3,\*</sup>, Ryoya Ishihara <sup>1</sup>, Hiroko Kominami <sup>1</sup>, Vadim Bakhmetyev <sup>3</sup>, Maxim Sychov <sup>3</sup>, Toru Aoki <sup>1,4</sup> and Hisashi Morii <sup>4</sup>

<sup>1</sup> Research Institute of Electronics, Shizuoka University, Japan

<sup>2</sup> Graduate School of Science and Technology, Shizuoka University, Japan

<sup>3</sup> Saint-Petersburg State Institute of Technology, St. Petersburg, Russia; office@technolog.edu.ru

<sup>4</sup> ANSeeN Inc., Japan

\* Correspondence: nastya.dorokhina@mail.ru

**Abstract:** The purpose of this experiment was the synthesis of a nanophosphor for medical use, namely in photodynamic therapy. Particular attention has been paid to obtaining nanosized particles with a suitable morphology. For this, the synthesis was carried out in various media (ethanol and ethylene glycol). The influence of stabilizers on the surface charge of particles is also studied. In this study, polyethylene glycol, polyethyleneimine, polyvinylpyrrolidone were used as stabilizers.

**Keywords:** X-ray luminescence; solvothermal synthesis; LaF<sub>3</sub>:Ce; Zeta-potential; PEG; PVP; PEI

## 1. Introduction

Fluorides have many advantages as fluorescent raw materials due to their low phonon energy and high ionicity [1]. Compared to oxide luminescent materials, rare earth fluorides have optical clarity, low vibrational energy, minimal dopant ion excited state quenching, and are also less prone to staining due to the formation of hole centers under the action of an ionizing emitter [2]. Fluoride nanocrystals doped with rare earth ions are of great interest due to their potential applications in lighting and displays [3–7], boost converters [8,9], biological fluorescent labels [10,11], transparent glass [12], scintillators [13], optical amplifiers [14], solar cell amplification [15] and photodynamic therapy [16,17]. Recently, some researchers have devoted themselves to the development of LaF<sub>3</sub> nanocrystals doped with rare earth ions due to their high photochemical stability, low toxicity and biocompatibility. In addition, their luminescent properties, including sharp absorption and emission lines and long lifetimes, are almost independent of particle size and can be tuned through doping with various lanthanide ions [18]. Ce<sup>3+</sup> is a strong emitter with a nanosecond luminescence lifetime that is shorter than rare earth elements with 4f configurations due to the allowed 5d-4f optical transition, which is independent of crystal field state mixing due to its dipole nature. Although the ion–lattice interaction for the 5d configuration is higher than for the 4f configuration, nonradiative decay with multiphonon emission is impossible due to the large distance between the 5d band and the nearest 4f level [19–21]. LaF<sub>3</sub>, which has a large band gap (according to various sources: from 6.04 eV [22] to 10.1 eV [23]), is an ideal host for studying Ce<sup>3+</sup> fluorescence for scintillators, since the 4f and 5d levels of cerium are located in the gap receiving grid. In addition, interactions between optically active Ce<sup>3+</sup> ions can decrease when these ions are replaced by La<sup>3+</sup> ions, which have very similar physical and chemical properties but are not optically active [24].

Agglomeration of LaF<sub>3</sub> nanocrystals doped with lanthanide ions is very common; firstly, because of the reduced open surface in nanocrystals which reduces surface energy, and secondly, as a rule, nanocrystals that do not have a special coating have a surface charge closer to neutral, which leads to aggregation and flocculation of particles due to the action of van der Waals forces of attraction on them. This can lead to physical instability [25,26]. To increase biocompatibility, as well as to prevent

agglomeration, the particles are coated with various stabilizers. The most widely used and studied stabilizer is polyethylene glycol (PEG). The process of applying a PEG coating to biomaterials to impart a latent characteristic is commonly referred to as PEGylation. It is now well known that PEGylation has many attractive properties; for example, it has been shown to increase the half-life of a drug in the body, prolonging its potency and thus reducing dosing frequency. The ability of PEG to prolong carrier circulation time is due mainly to its physical properties, which, in turn, can reduce or prevent protein absorption. It has been approved by the FDA for use in a variety of dosage forms. PEGylation remains the reference process for the development of biologically relevant systems with in vivo characteristics. However, the disadvantages of this stabilizer have also become known: a long elimination time, lack of biodegradability, formation of undesirable by-products, and mechanical degradation [27]. Alternatively, polyethyleneimine and polyvinylpyrrolidone have also been successfully used as stabilizers.

This study is related to the improvement of the parameters of the process used for the synthesis of  $\text{LaF}_3$  nanocrystals by the solvothermal method. The influence of the reaction medium and stabilizers on the structural, morphological and surface properties were studied using appropriate mathematical and analytical methods. After that,  $\text{Ce}^{3+}$  ions of the optimal concentration were doped into the optimal host nanomaterial, and the optical characteristics for medical applications were studied.

## 2. Materials and Methods

A series of fluoride phosphors with the composition  $\text{LaF}_3:\text{Ce}^{3+}$  4...6%mol. was synthesized. A typical synthesis [28] was carried out in ethylene glycol or ethanol. Water solution of cerium and lanthanum chlorides (8 mmol) was well mixed and added to ethylene glycol. After adding stabilizer polyethylene glycol Mw = 20000 (PEG-20000), the mixture was vigorously stirred on a magnetic stirrer at room temperature. Ammonium fluoride  $\text{NH}_4\text{F}$  (12 ml of 110 mmol solution) was dissolved in ethylene glycol or water, and added to the above solution, and again stirred vigorously at room temperature for 30 minutes. Finally, the mixture was transferred to a Teflon liner, placed in a sealed stainless steel autoclave, where it was subjected to a solvothermal treatment at  $200^\circ\text{C}$  for 4 hours, and cooled naturally to room temperature. The precipitate was washed in ethanol and deionized water several times, and the final products were dried at  $40^\circ\text{C}$  for 6 hours in a normal atmosphere. To determine the most suitable stabilizer that will prevent particle coalescence and ensure biocompatibility, we are implementing a one-stage hydrothermal synthesis of  $\text{LaF}_3:\text{Ce}^{3+}$  nanocrystals with various organic surfactants, in particular, polyethylene glycol (PEG-200, PEG-2000, PEG-20.000), polyethyleneimine (PEI Mw 60,000-80,000), polyvinylpyrrolidone (PVP Mw 1,300,000) and investigating the luminescent and surface properties of nanoparticles. All samples have a cerium concentration of 5%mol.

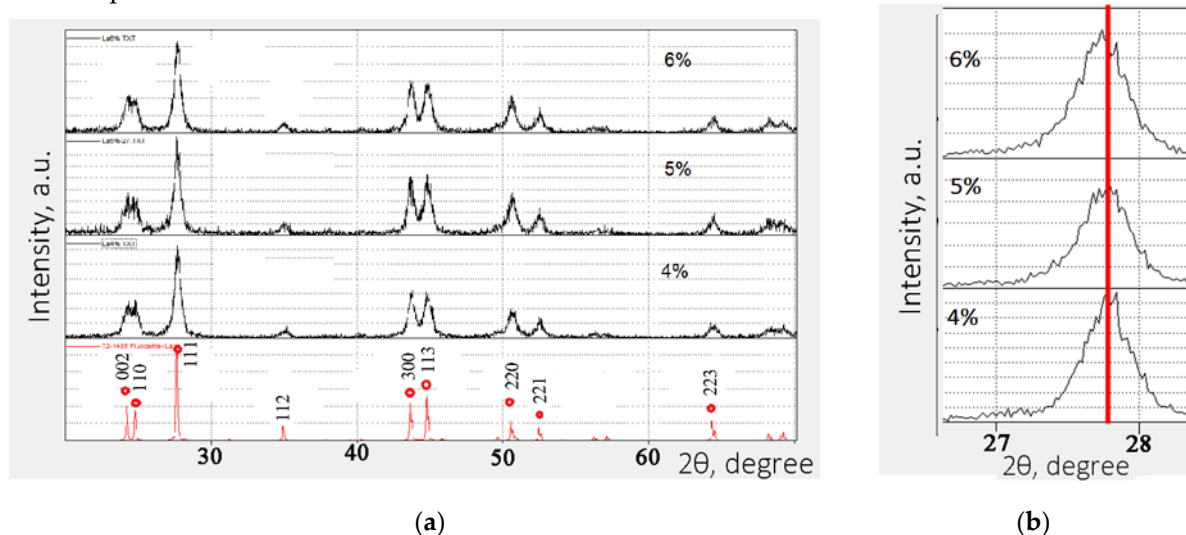
The structural characteristics of the final products were investigated by powder X-ray diffraction (XRD) using Cu-K $\alpha$  radiation ( $\lambda = 0.15405$  nm) on a Rigaku-RINT2200 diffractometer. The morphology and size of the obtained samples were observed using field emission scanning electron microscope (FE-SEM, JSM-7001F, JEOL). The emission spectra of ultraviolet and visible photoluminescence were recorded using a laboratory setup - a spectrofluorometer with two monochromators (model of an ultramonochromatic light source) equipped with a xenon lamp as an exciter. The obtained spectra were analyzed by deconvolution into Gaussian bands. The X-ray luminescence spectra were measured on a laboratory setup with a copper anode at a voltage of 80 kV and a current of 62 mA. The decay time was measured with a Hamamatsu compact fluorescence lifetime spectrometer 11367 (TR 50 ns, frequency 10000 MHz). FTIR spectrum is recorded between 4000 and  $400\text{ cm}^{-1}$ . Dried samples were measured with FT/IR-6300, JASCO. Surface charge and size distribution of the samples were measured with Zetasizer Ultra and analyzed with ZS Xplorer software by Malvern Pnalytical. All measurements were carried out at room temperature.

## 3. Results and Discussion

To determine the optimal concentration of cerium, a series of syntheses of samples with a concentration of 4...6 mol% was carried out. Figure 1 shows the XRD patterns of the obtained samples. The structure of the obtained  $\text{LaF}_3:\text{Ce}^{3+}$  nanoparticles is in good agreement with the hexagonal structure of bulk  $\text{LaF}_3$  (card 72-1435). The diffraction peaks for all samples are broadened, which indicates the nanocrystalline nature of the samples. The average crystallite sizes were estimated from the Scherrer equation [29],

$$D_{hkl} = k\lambda/\beta\cos\Theta$$

where  $k = 1$ ,  $\lambda = 0,154184$  nm represents the wavelength of Cu  $K$  radiation,  $\Theta$  is the angle of the X-ray diffraction peak, and  $\beta$  represents the corrected half width of the diffraction peak. Taking the eight main peaks (002, 110, 111, 112, 300, 113, 220, 221, 223), the average crystallite sizes of  $\text{LaF}_3:4\%\text{Ce}^{3+}$ ,  $\text{LaF}_3:5\%\text{Ce}^{3+}$  and  $\text{LaF}_3:6\%\text{Ce}^{3+}$  are about 25.1, 31.9 and 33.1 nm, respectively. Figure 1-b shows the peak (111) at  $2\Theta = 27.6^\circ$ , it can be seen that with an increase in the concentration of cerium, the peak will shift towards lower degrees, which indicates an increase in the amount of the cerium fluoride phase.



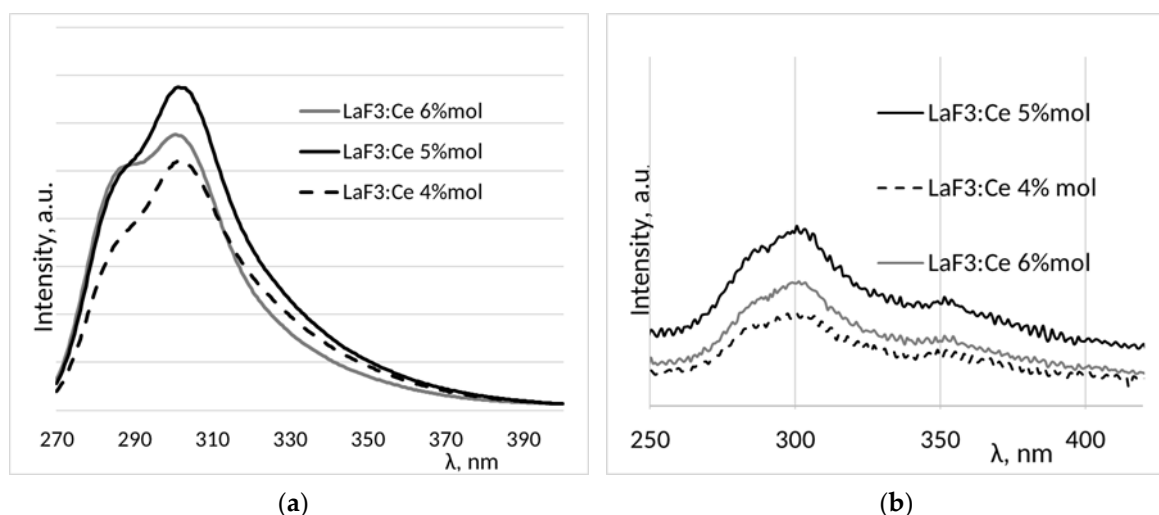
**Figure 1.** XRD patterns of  $\text{LaF}_3:\text{Ce}$ : (a) - with different  $\text{Ce}^{3+}$  concentration; (b) – XRD peak (111) at  $27.6^\circ$ .

Figure 2 shows the Photo and X-ray luminescence spectra of  $\text{LaF}_3:\text{Ce}$  phosphors with different activator concentrations. Photoluminescence was measured at room temperature with an excitation wave of 255 nm (Figure 2(a)).

Broadband radiation in the region from 270 to 400 nm and peaking at 300 nm can be attributed to the  $5d-4f$  transition of  $\text{Ce}^{3+}$ . With an increase in the doping concentration of  $\text{Ce}^{3+}$ , the radiation intensity gradually increases, reaching a maximum at a concentration of 5%mol., and then decreases. The decrease in the radiation intensity is related to the concentration effect of quenching at a higher doping concentration of  $\text{Ce}^{3+}$ . A similar behavior is also observed upon X-ray excitation (Figure2(b)).

It is known that the luminescence spectra of trivalent lanthanide ions in crystals are mainly due to two types of electronic transitions: the  $4f-4f$  transition and the  $5d-4f$  transition. The excited electronic configuration of  $\text{Ce}^{3+}$  has the form  $5d^1$  and it is not shielded from the surroundings. The  $5d$  electron interacts strongly with neighboring anion ligands in compounds, which leads to broadband emission. The  $4f$  orbital is shielded from the environment by the filled  $5s^2$  and  $5p^6$  orbitals. Therefore, the effect of the main lattice on optical transitions within the  $4f^n$  configuration is small [30].





**Figure 2.** Photo-luminescent (a) and X-Ray luminescent spectra of LaF<sub>3</sub>:Ce with different Ce<sup>3+</sup> concentration.

It is important to use the correct technique to synthesize nanoparticles for a medical application because each nanoparticle must have the appropriate morphology for the desired application. It is known that toxicity increases from spherical to acicular particles [31]. Therefore, it is very important to synthesize nanosized particles, and also, if possible, to produce their ideal shape. We thought that solvothermal methods would control the morphology to an appropriate degree. When conducting a solvothermal reaction, many factors must be taken into account, such as the concentrations of the reactants, the solubility of the reactants, the reaction temperature, the reaction time, the choice of solvent, and the pressure, all of which can be varied. In our previous papers, we have already discussed the optimal parameters for the synthesis of yttrium fluoride [32]. In this article, we paid special attention to the solvent used as the reaction medium. In this case, we used ethanol and ethylene glycol (EG).

The solvothermal reaction was carried out at 200°C for 4 h using PEG-20000 as a stabilizer and with cerium concentration 5%mol. As a result of synthesis using these reaction media, pure hexagonal lanthanum fluoride was obtained (Figure 3). Thus, it can be concluded that the synthesis medium does not affect the formation of the phase. This statement was also confirmed to us in the work [32].

Figures 4 and 5 show SEM images and size distribution histograms calculated from the acquired images, respectively.

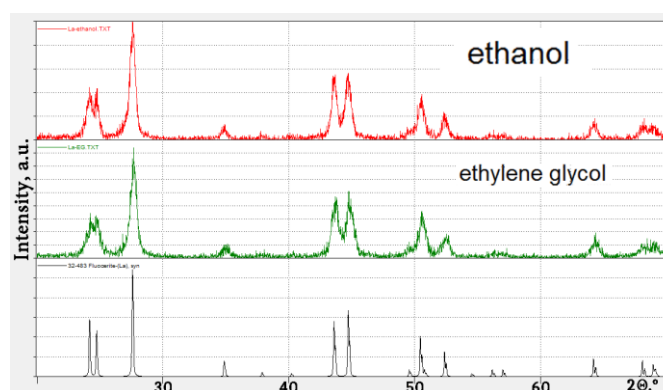


**Figure 3.** XRD patterns of LaF<sub>3</sub>:Ce synthesized in various media.

SEM images (Figure 4) display that the obtained particles are oval in shape and do not exceed nanosize. These samples are also histograms in Figure 5, which were read from the acquired images using the software. It should be noted that the synthesis medium has practically no effect on the particle morphology, however, a narrower particle size distribution was obtained as a result of

synthesis in an ethanol medium. Also, in this medium, as calculations show, it is possible to obtain an average particle size of about 30 nm, while in an ethylene glycol (EG) medium the average size is about 45 nm. Thus, ethanol was chosen as the reaction medium for the solvothermal synthesis of lanthanum fluoride.

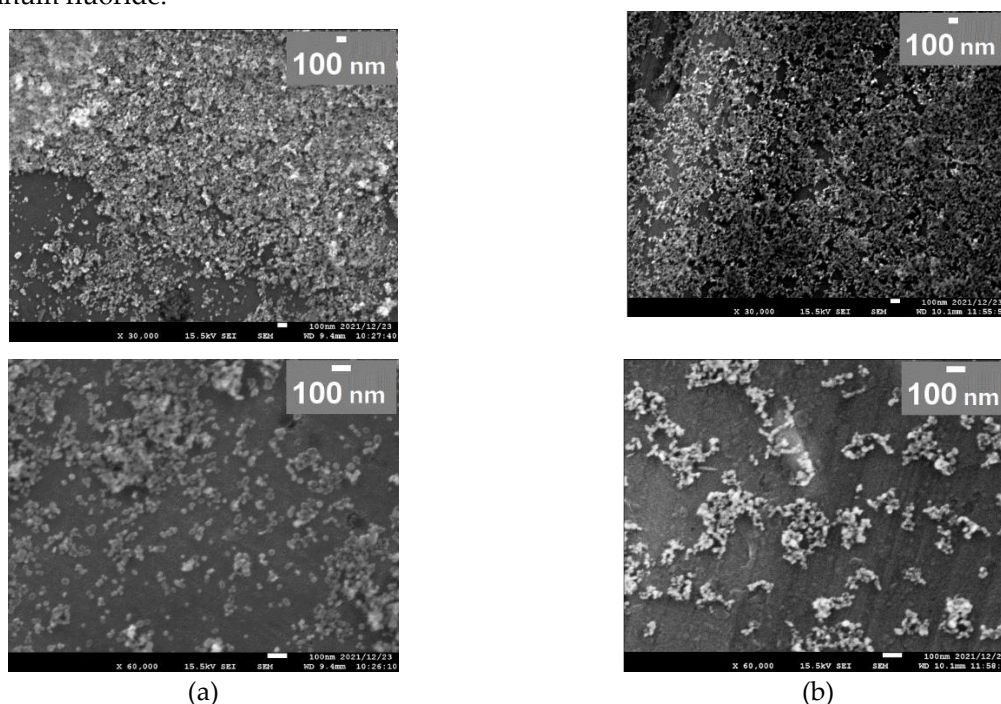


**Figure 4.** SEM images of LaF<sub>3</sub>:Ce 5%mol. synthesized in Ethanol (a) and EG (b).

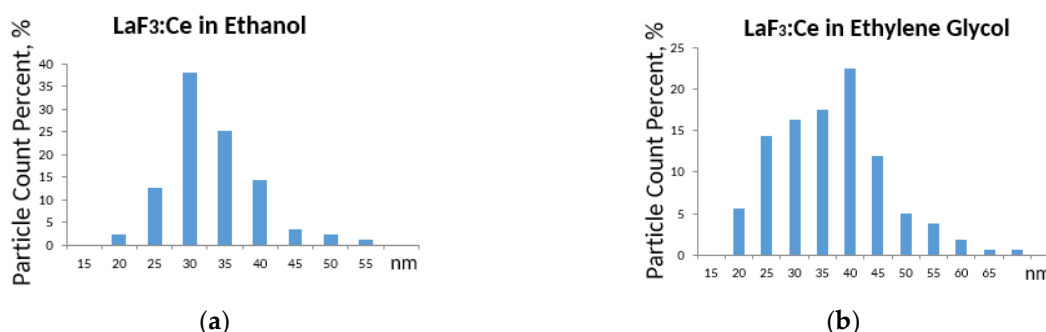
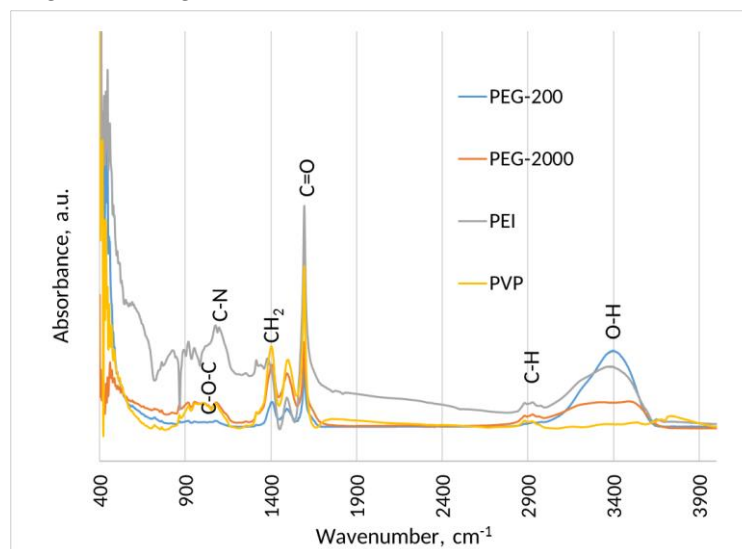


**Figure 5.** Size distribution of LaF<sub>3</sub>:Ce 5%mol. synthesized in Ethanol (a) and EG (b).

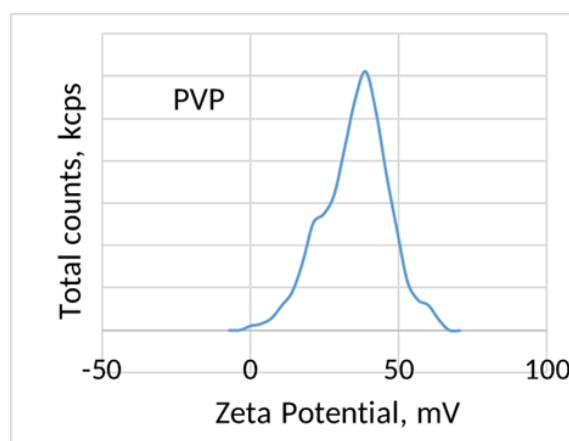
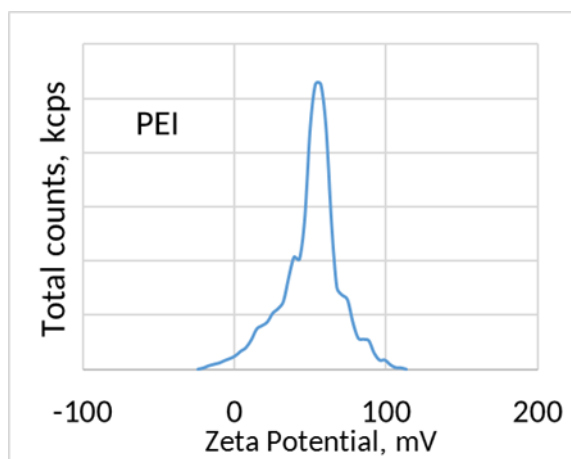
Reducing the particle size increases the number of surface atoms and the surface energy of the resulting particles, so these nanoparticles must be stabilized with suitable compounds [33]. The stabilization of nanoparticles is carried out before their actual use in any technological applications by modifying their surface with appropriate stabilizers. This surface modification with stabilizers (also called capping ligands) is critical to achieving sufficient repulsive forces between particles that prevent particle aggregation and help obtain a stable suspension of particles. A special polymer coating allows for higher biocompatibility, prevents agglomeration, and also makes it possible to obtain a stable colloidal nanosuspension. We synthesized a series of samples with various stabilizers: polyethylene glycol (PEG) with Mw 200 and 2000, polyvinylpyrrolidone (PVP) and polyethyleneimine (PEI). At present, the control of the morphology and size of fluoride nanoparticles during their preparation is an important factor that needs to be addressed for their use in medicine.

The functional groups of the powders were identified using FT-IR as shown in Figure 6. A broad absorption band around 3500-3400 cm<sup>-1</sup> refers to stretching vibrations (-OH). In the spectrum of PEG200 and PEG2000, characteristic bands of certain functional groups were found, such as a band at 2874.2 cm<sup>-1</sup> belonging to the -CH group [34] and a band at 1103.9 cm<sup>-1</sup> belonging to the -C-O-C

group [35]. These two characteristic bands and some other bands near  $1103.9\text{ cm}^{-1}$  also appear in the PEG-  $\text{LaF}_3\text{:Ce}$  spectrum, indicating successful conjugation of PEG to the  $\text{LaF}_3\text{:Ce}$  surface. The spectrum of PEI shows weak peaks in the  $1170\text{--}1050\text{ cm}^{-1}$  range that correspond to C-C, C-O-C and C-O (in alcohols) stretching vibrations (associated with carbo-hydrate ring), and C-N stretching. The second sharp peak is observed in the wavenumber range  $1632\text{--}1622\text{ cm}^{-1}$ ; this large band may be assigned to C=O asymmetric stretching in (COO-), (-N-H) bending vibration (for primary and secondary amines) and/or open-chain imino groups (-C=N-). In addition, stretching vibrations of -CH bonds are appearing in the region  $2980\text{--}2850\text{ cm}^{-1}$  confirming the expected presence of linear aliphatic chains. The spectrum of PVP has characteristic peaks C=O ( $1660\text{ cm}^{-1}$ ) and C-N ( $1290\text{ cm}^{-1}$ ), which confirms the functionalization of PVP lanthanum fluoride nanoparticles through intermolecular hydrogen bonding.



**Figure 6.** FT-IR spectra of  $\text{LaF}_3\text{:Ce}$  with different stabilizers.



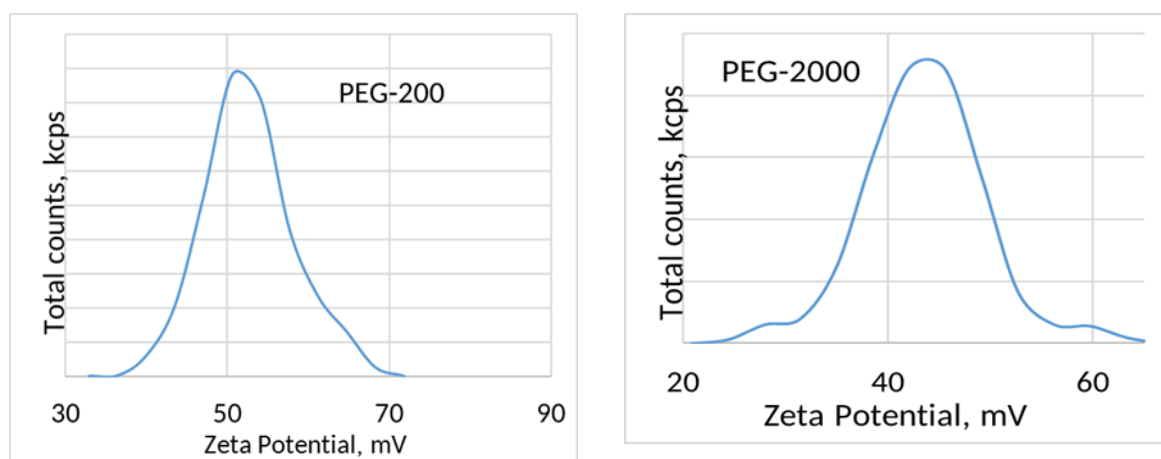


**Figure 7.** Zeta-potential of LaF<sub>3</sub>:Ce 5%mol with different stabilizers.

Particles with zeta potential of  $\pm 30$  mV have an optimal surface charge, which is acceptable for biocompatibility [36]. Zeta potential values are typically in the range of +100 to -100 mV. The high value of the zeta potential of nanocrystals indicates a good physical stability of nanosuspensions due to the electrostatic repulsion of individual particles. A zeta potential value other than -30 mV to +30 mV is generally considered to have sufficient repulsive force to achieve better physical colloidal stability. On the other hand, a low zeta potential can lead to aggregation and flocculation of particles due to attractive Van der Waals forces on them, which can lead to physical instability [37].

As can be seen from Figure 7, PEG-coated particles have an extremely positive charge, which can be as high as 70 mV. In the case of PEI, the particles have both positive and negative charges, which directly leads to a high probability of agglomeration. PVP has positively charged particles, most of which have a charge of about 40 mV, which is close to the optimum particle charge to achieve colloidal stability. Therefore, PVP was chosen as a suitable stabilizer.

After determining the optimal surfactant, an experiment was conducted to determine the optimal amount of PVP. Four samples were synthesized with different PVP amount: 0 g, 0.375 g, 0.75 g and 1.5 g. Figure 8(a) shows the diffraction patterns of the obtained samples. As noted earlier, the presence of surfactants does not affect the phase composition. Therefore, it is possible to observe hexagonal lanthanum and cerium fluoride without impurity phases.

Figure 8(b) shows the excitation and luminescence spectra of the obtained samples. Peaks located in the region of 90-150 nm are related to excitation of the phosphor host - lanthanum fluoride. As can be seen from the excitation spectra, the main peaks, in contrast to the emission spectra, are bifurcated. We have a hypothesis to explain this phenomenon – that the particles of these samples are nanosized. Similar results have already been observed in [38]. The emission spectra of the obtained samples demonstrate the same pattern as for the samples obtained earlier. The sample with a PVP content of 0.75 g has the highest intensity.



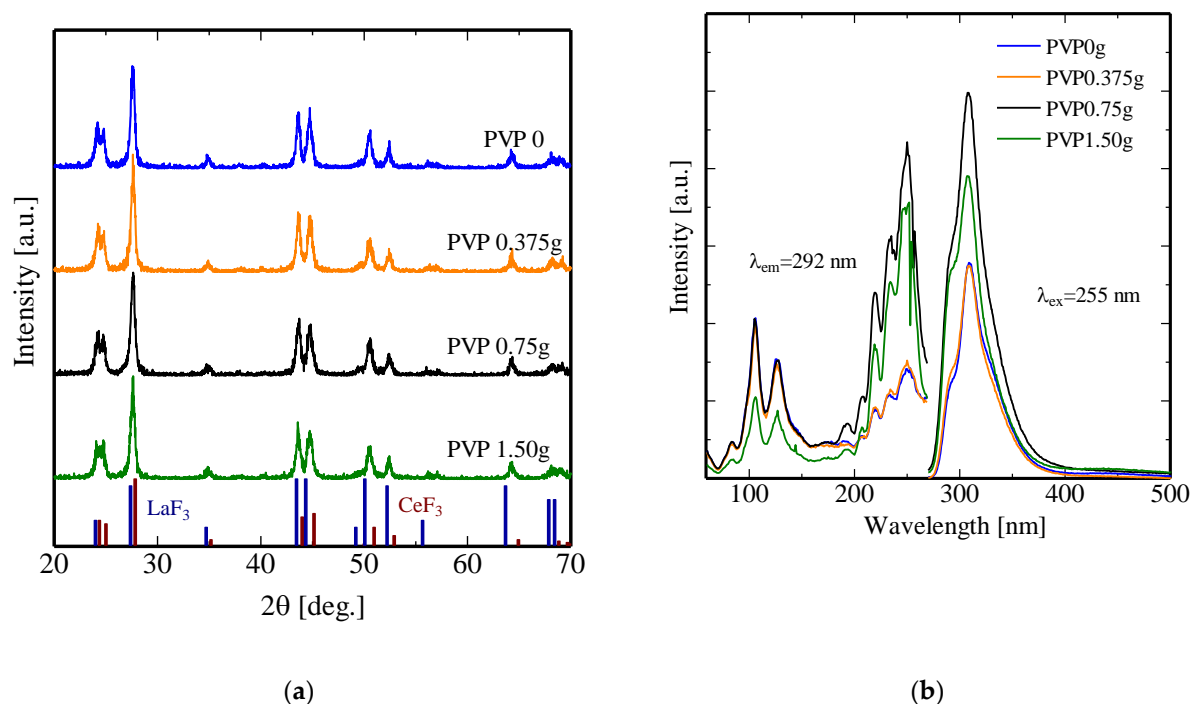


**Figure 8.** XRD patterns (a) and photoluminescent spectra of  $\text{LaF}_3\text{:Ce}$  with different amount of PVP.

#### 4. Conclusions

$\text{LaF}_3$  nanoparticles doped with cerium ( $\text{Ce}^{3+}$ ) at a concentration of 4...6 mol.% were synthesized by the solvothermal method in various media: ethanol and ethylene glycol. Ethanol was chosen as the optimal reaction medium for the synthesis, and the sample with a cerium concentration of 5 mol % exhibits the highest intensity upon UV and X-ray excitation. In this synthesis procedure, polyethylene glycol, polyvinylpyrrolidone, and polyethyleneimine were used as stabilizers that bind to the surface of the particle, limiting the growth of the nanoparticles. The average particle size of the resulting nanoparticles is 30 nm, and these particles can be dispersed in water to form a colloidal solution. Due to their low toxicity, water-soluble luminescent  $\text{LaF}_3\text{:Ce}$  nanoparticles can be used in future biological experiments.

**Author Contributions:** Conceptualization, Dorokhina A.M., Kominami H. and Sychov M.M.; methodology, Kominami H., Bakhmetyev V.V. and Dorokhina A.M.; investigation, Dorokhina A.M., Ishihara R., Kominami H.; resources, Kominami H., Aoki T., Morii H.; writing—original draft preparation, Dorokhina A.M.; writing—review and editing, Kominami H. All authors have read and agreed to the published version of the manuscript.

**Acknowledgments:** This work was partly supported by a MEXT scholarship.

**Conflicts of Interest:** The authors declare no conflict of interest.

#### References

1. R. X. Yan and Y. D. Li / Down/Up Conversion in  $\text{Ln}^{3+}$ -Doped  $\text{YF}_3$  Nanocrystals // *Adv. Funct. Mater.* 15, 763 (2005).
2. M. C. Tan, L. Al-Baroudi, and R. E. Riman / Surfactant effects on efficiency enhancement of infrared-to-visible upconversion emissions of  $\text{NaYF}_4\text{:Yb-Er}$  // *Appl. Mater. Interfaces* 3, 3910-5 (2011).
3. Z. L. Wang, H. L. W. Chan, H. L. Li, and J. H. Hao / Highly efficient low-voltage cathodoluminescence of  $\text{LaF}_3\text{:Ln}^{3+}$  ( $\text{Ln}=\text{Eu}^{3+}, \text{Ce}^{3+}, \text{Tb}^{3+}$ ) spherical particles // *Appl. Phys. Lett.* 93, 141106 (2008).
4. P.Y. Jia, J. Lin, M. Yu / Sol-gel deposition and luminescence properties of  $\text{LiYF}_4\text{:Tb}^{3+}$  thin films // *Journal of Luminescence*, Volumes 122–123, 2007, Pages 134-136

5. Doan Thi Tuyet, Vu Thi Hong Quan, Bartosz Bondzior, Przemysław Jacek Dereń, Ravi Teja Velpula, Hieu Pham Trung Nguyen, Luu Anh Tuyen, Nguyen Quang Hung, and Hoang-Duy Nguyen / Deep red fluoride dots-in-nanoparticles for high color quality micro white light-emitting diodes // *Opt. Express* 28, 26189-26199 (2020)
6. Kemnitz, E., Mahn, S. & Krah, T. / Nano metal fluorides: small particles with great properties // *ChemTexts* 6, 19 (2020).
7. Zewei Quan, Dongmei Yang, Piaoping Yang, Xiaoming Zhang, Hongzhou Lian, Xiaoming Liu, and Jun Lin / Uniform Colloidal Alkaline Earth Metal Fluoride Nanocrystals: Nonhydrolytic Synthesis and Luminescence Properties // *Inorg. Chem.* 2008, 47, 20, p. 9509–9517.
8. S. Heer, K. Kümpe, H.-U. Gudel, and M. Haase / Highly Efficient Multicolour Upconversion Emission in Transparent Colloids of Lanthanide-Doped NaYF<sub>4</sub> Nanocrystals // *Adv. Mater.* 16, 2102 (2004).
9. S. Schietinger, L. S. Menezes, B. Lauritzen, and O. Benson / Observation of Size Dependence in Multicolor Upconversion in Single Yb<sup>3+</sup>, Er<sup>3+</sup> Codoped NaYF<sub>4</sub> Nanocrystals // *Nano Lett.* 9, 2477–2481 (2009).
10. G. S. Yi, H. C. Lu, S. Y. Zhao, Y. Ge, W. J. Yang, D. P. Chen, and L. H. Guo / Synthesis, Characterization, and Biological Application of Size-Controlled Nanocrystalline NaYF<sub>4</sub>:Yb,Er Infrared-to-Visible Up-Conversion Phosphors // *Nano Lett.* 4, 2191–2196 (2004).
11. Nam SH, Bae YM, Park YI, Kim JH, Kim HM, Choi JS, Lee KT, Hyeon T, Suh YD / Long-term real-time tracking of lanthanide ion doped upconverting nanoparticles in living cells // *Angew Chem Int Ed Engl.* 2011 Jun 27;50(27):6093-7
12. S. F. Zhou, N. Jiang, K. Miura, S. Tanabe, M. Shimizu, M. Sakakura, Y. Shimotsuma, M. Nishi, J. R. Qiu, and K. Hirao / Simultaneous Tailoring of Phase Evolution and Dopant Distribution in the Glassy Phase for Controllable Luminescence // *J. Am. Chem. Soc.* 132,17945–17952 (2010).
13. Z. L. Wang, Z. W. Quan, P. Y. Jia, C. K. Lin, Y. Luo, Y. Chen, J. Fang, W. Zhou, C. J. O'Connor, and J. Lin / Cerium (III) Fluoride Thin Films by XPS // *Chem. Mater.* 18, 2030 (2006).
14. S. Sivakumar, F. C. J. M. van Veggel, and M. Raudsepp / Bright White Light through Up-Conversion of a Single NIR Source from Sol-Gel-Derived Thin Film Made with Ln<sup>3+</sup>-Doped LaF<sub>3</sub> Nanoparticles // *J. Am. Chem. Soc.* 127, 36, 12464–12465 (2005).
15. Liu, Shu-Man; Chen, Wei; Wang, Zhan-Guo / Luminescence Nanocrystals for Solar Cell Enhancement // *Journal of Nanoscience and Nanotechnology*, Volume 10, Number 3, March 2010, pp. 1418-1429(12)
16. Y. F. Liu, W. Chen, S. P. Wang, and A. G. Joly / Investigation of water-soluble x-ray luminescence nanoparticles for photodynamic activation // *Appl. Phys. Lett.* 92, 043901 (2008).
17. Chen, Wei / Nanoparticle Self-Lighting Photodynamic Therapy for Cancer Treatment // *Journal of Biomedical Nanotechnology*, V. 4(4), 2008, p. 369-376(8)
18. Wang F, Han Y, Lim CS, Lu Y, Wang J, Xu J, Chen H, Zhang C, Hong M, Liu X / Simultaneous phase and size control of upconversion nanocrystals through lanthanide doping // *Nature.* 2010 Feb 25;463(7284):1061-5
19. W.W. Moses, S.E. Derenzo, M.J. Weber, A.K. Ray-Chaudhuri, F. Cerrina / Scintillation mechanisms in cerium fluoride, *Journal of Luminescence* // Volume 59, Issues 1–2, 1994, Pages 89-100.
20. M. Yao, A. G. Joly, and W. Chen / Formation and Luminescence Phenomena of LaF<sub>3</sub>:Ce<sup>3+</sup> Nanoparticles and Lanthanide–Organic Compounds in Dimethyl Sulfoxide // *J. Phys. Chem. C* 2010, 114, 2, 826–831 (2010).
21. M. D. Birowosuto, P. Dorenbos, C. W. E. van Eijk, K. W. Krmer, and H. U. Gudel / Scintillation properties and anomalous Ce<sup>3+</sup> emission of Cs<sub>2</sub>NaREBr<sub>6</sub>:Ce<sup>3+</sup> (RE = La,Y,Lu) // *J. Phys.: Condens. Matter* 18, 6133 (2006).

22. Petousis, I., Mrdjenovich, D., Ballouz, E. et al. / High-throughput screening of inorganic compounds for the discovery of novel dielectric and optical materials // *Sci Data* 4, 160134 (2017).
23. Tabatabaee, F., Sabbagh Alvani, A.A., Sameie, H. et al. / Ce<sup>3+</sup>-doped LaF<sub>3</sub> nanoparticles: Wet-chemical synthesis and photo-physical characteristics "optical properties of LaF<sub>3</sub>:Ce nanomaterials // *Met. Mater. Int.* 20, 169–176 (2014).
24. A. Canning, A. Chaudhry, R. Boutchko, and N. Gronbeck- Jensen / First-principles study of luminescence in Ce-doped inorganic scintillators // *Phys. Rev.* Vol. 83, Iss. 12 , 125115 (2011).
25. Chrysanthia Freitas, Rainer H. Müller / Spray-drying of solid lipid nanoparticles (SLNTM) // *European Journal of Pharmaceutics and Biopharmaceutics*, Volume 46, Issue 2, 1998, Pages 145-151,
26. Shah S, McRae AF, Marioni RE, Harris SE, Gibson J, Henders AK, Redmond P, Cox SR, Pattie A, Corley J, Murphy L, Martin NG, Montgomery GW, Starr JM, Wray NR, Deary IJ, Visscher PM / Genetic and environmental exposures constrain epigenetic drift over the human life course // *Genome Res.* 2014 Nov;24(11):1725-33
27. Fan Zhang, Mu-rong Liu , Hai-tong Wan / Discussion about Several Potential Drawbacks of PEGylated Therapeutic Proteins // *Biological and Pharmaceutical Bulletin*, 2014 V. 37(3), P. 335-339
28. L. Sudheendra, Gautom K. Das, Changqing Li, Daniel Stark, Jake Cena, Simon Cherry, Ian M. Kennedy / NaGdF<sub>4</sub>:Eu<sup>3+</sup> Nanoparticles for Enhanced X-ray Excited Optical Imaging // *Chem. Mater.* 26, 2014, p. 1881–1888.
29. V.S. Vinila, Jayakumari Isac, Design, Fabrication, and Characterization of Multifunctional Nanomaterials, Elsevier, 2022.
30. Hai Guo, Tian Zhang, Yan Min Qia<sup>1</sup>, Lei Hong Zhao, and Zheng Quan Li / Ionic Liquid-Based Approach to Monodisperse Luminescent LaF<sub>3</sub>:Ce,Tb Nanodiskettes: Synthesis, Structural and Photoluminescent Properties // *Journal of Nanoscience and Nanotechnology*, Vol. 10, p. 1913–1919, 2010.
31. Kouichi NAKASHIMA, Shintaro UENO, Satoshi WADA // Solvothermal synthesis of KNbO<sub>3</sub> nanocubes using various organic solvents / *Journal of the Ceramic Society of Japan* 2014 Volume 122 Issue 1427 Pages 547-551.
32. A M Dorokhina et al / Study of the properties of Ce<sup>3+</sup>-doped fluoride nanophosphors: phase composition, morphology, luminescence // *J. Phys.: Conf. Ser.* 2056 012048, 2021, p.1-8.
33. R. G. Chaudhuri , S. Paria / Core/Shell Nanoparticles: Classes, Properties, Synthesis Mechanisms, Characterization, and Applications // *Chem. Rev.* 2012, 112, 4, p. 2373–2433.
34. Mu H, Wang X, Lin PH, Yao Q, Chen C / Chlorotyrosine promotes human aortic smooth muscle cell migration through increasing superoxide anion production and ERK1/2 activation // *Atherosclerosis.* 2008;201(1):67–75.
35. Petersen H, Fechner PM, Martin AL, et al / Polyethylenimine-graftpoly(ethylene glycol) copolymers: influence of copolymer block structure on DNA complexation and biological activities as gene delivery system // *Bioconj Chem.* 2002;13(4):845–854.
36. Shabnam Samimi, Niloufar Maghsoudnia, Reza Baradaran Eftekhari, Farid Dorkoosh, Chapter 3 - Lipid-Based Nanoparticles for Drug Delivery Systems, Editor(s): Shyam S. Mohapatra, Shivendu Ranjan, Nandita Dasgupta, Raghvendra Kumar Mishra, Sabu Thomas, In *Micro and Nano Technologies, Characterization and Biology of Nanomaterials for Drug Delivery*, Elsevier, 2019, Pages 47-76.
37. Emil Joseph, Gautam Singhvi, Chapter 4 - Multifunctional nanocrystals for cancer therapy: a potential nanocarrier, Editor(s): Alexandru Mihai Grumezescu, *Nanomaterials for Drug Delivery and Therapy*, William Andrew Publishing, 2019, Pages 91-116.

38. CHEN Yan-Ping, LUO De-Li, XU Qin-Ying, YANG Suo-Long, TANG Tao, WANG Xiao-Ying /无机材料学报 Structure and Fluorescence Quenching of Li<sub>2</sub>O-MgO-Al<sub>2</sub>O<sub>3</sub>-SiO<sub>2</sub> Glasses Doped with Trivalent Cerium // 2014, 29(9): 967-971.

**Disclaimer/Publisher's Note:** The statements, opinions and data contained in all publications are solely those of the individual author(s) and contributor(s) and not of MDPI and/or the editor(s). MDPI and/or the editor(s) disclaim responsibility for any injury to people or property resulting from any ideas, methods, instructions or products referred to in the content.